Conversion of Mitochondrial Cytochrome b_5 into A Species Capable of Performing the Efficient Coupled Oxidation of Heme†

Juan Carlos Rodríguez and Mario Rivera*

Department of Chemistry, Oklahoma State University, Stillwater, Oklahoma 74078-3071

Received April 24, 1998; Revised Manuscript Received July 29, 1998

ABSTRACT: Histidine-63, one of the heme axial ligands in outer mitochondrial membrane cytochrome b_5 (OM cyt b_5) has been replaced by a methionine. The H63M variant performs the efficient and regioselective coupled oxidation of heme in order to produce >90% of the α-isomer of verdoheme. The variant was characterized by electronic, EPR, and NMR spectroscopic studies which indicate that the ferric form is a high-spin species whose heme is coordinated by histidine-39 in the proximal site and likely by water in the distal site. The coordination of methionine to the ferric heme was ruled out on the basis of NMR spectroscopic studies. Addition of imidazole to a solution of the ferric variant results in the formation of a species axially coordinated by imidazole and histidine-63. The reduction potential of the variant was found to be +110 mV in the absence of exogenous imidazole and −92 mV in the presence of imidazole. These values compare well with the reduction potential of myoglobin (50 mV) and wild-type OM cyt b_5 (−102 mV), respectively, consistent with the axial ligation described above. The ferrous variant, on the other hand, is a low-spin species coordinated by histidine-39 and methionine-63. Carbon monoxide (CO) readily displaces Met-63 from its coordination site on the ferrous heme, whereas CO cannot completely displace Met-63 from its coordination site on verdoheme. Consequently, the mechanism of inhibition for the oxidation of verdoheme to iron-biliverdin in the H63M variant appears to be similar to that observed for the heme−heme oxygenase complex in the presence of CO.

Heme-containing proteins play a crucial role in maintaining life in essentially all living organisms. Examples of these proteins include the oxygen carriers hemoglobin and myoglobin, in which the heme active center is used by the protein as an oxygen-binding site. Cytochromes, on the other hand, are electron-transfer heme proteins in which the heme active site is shuttled between different oxidation states in order to accept or donate electrons (cytochrome b_5, cytochrome *c*). Heme-containing enzymes are also capable of reacting with molecular oxygen to perform monooxygenation reactions (cytochrome P450) or react with peroxides to carry out peroxidase reactions (horseradish peroxidase, cytochrome *c* peroxidase). It is remarkable that despite the wide range of chemical functions displayed by heme-containing enzymes and proteins, they all share the same prosthetic group, protoheme IX. Important properties such as the reduction potential and reactivity exhibited by the heme active site in several different heme proteins are modulated by the structural characteristics encountered in their heme-binding cavities. One of the most significant structural characteristics governing the activity of hemoproteins is the coordination environment of the heme iron. For example, the heme in electron-transfer proteins is coordinated by two strongly coordinated axial ligands, and in general, these proteins do not bind molecular oxygen or peroxides. On the other hand, the heme in most other types of heme-containing proteins is coordinated by a proximal axial ligand, therefore, providing an accessible vacant distal site where molecular oxygen, peroxides, and other exogenous ligands can bind.

A large effort has been directed to understand the effect that changes in axial ligation have on the properties of heme proteins (*1*−*13*). Protein semisynthesis and, in particular, site-directed mutagenesis have been exploited to generate heme proteins with novel heme-axial ligation. For example, Raphael and Gray reported that replacement of methionine-80, a heme axial ligand in cytochrome *c*, with a histidine (*2*) or with a cysteine (*3*) results in heme proteins with reduction potentials similar to those displayed by microsomal cytochrome b_5 and cytochrome $P450_{cam}$, respectively. Horse heart myoglobin has been converted into an electron-transfer protein upon replacement of the distal valine-68 residue with a histidine. This resulted in a bis-histidine coordinated species with spectroscopic characteristics similar to those of cytochrome b_5 (*4*). Replacement of the proximal axial ligand of human myoglobin with cysteine resulted in a ferric species whose heme is coordinated by a proximal thiolate and whose spectroscopic characteristics are similar to those of cytochrome P450. In addition, the monooxygenase activity of the mutant was modestly increased (*7*, *8*).

This report presents evidence demonstrating that upon replacement of histidine-63 for methionine in the electron-transfer protein, outer mitochondrial membrane cytochrome b_5 (OM cyt b_5), a variant is produced that is capable of

† The financial support of grants from the National Institutes of Health (GM 50503) and the American Heart Association (9507904S) is gratefully acknowledged. Funds for the 600 MHz spectrometer of the Oklahoma Statewide Shared NMR facility were provided by the National Science foundation (BIR-9512269), the Oklahoma State Regents for Higher Education, W. W. Keck Foundation and Conoco, Inc.

* To whom correspondence should be addressed.

S0006-2960(98)00932-5 CCC: $15.00
Published on Web 09/05/1998

performing the efficient coupled oxidation of heme. The coupled oxidation of the heme in the H63M variant is arrested at the verdoheme stage and proceeds with >90% regioselectivity for the α-meso position. The only other example of a mutant protein capable of performing the efficient and regioselective coupled oxidation of heme is that reported for theV67A−V68S double variant of horse heart myoglobin (*14*).

EXPERIMENTAL SECTION

Site-Directed Mutagenesis, Protein Expression, and Purification. The transformer site-directed mutagenesis kit (Clonetech) and the recombinant plasmid MRL1 (*28*) were used to construct the mutants following a protocol outlined previously (*21*). The sequences corresponding to the mutagenic primers designed to introduce mutations H63M, H39M, and that corresponding to the selection primer (*Afl*III to *Bgl*II) are 5′-CCGAATCTTTCGAAGATGTTGGCATGTCTCCGGATGCGCG-3′, 5′-CCCGTTTCCTGTCTGAAATGCCGGGCGGCGAAGAAGTTCTGC-3′, 5′-GGGGATAACGCAGGAAAGAAGATCTGAGCAAAAGGCC-3′, respectively. The underlined codons represent mismatches introduced to generate the mutations.

The mutated gene was subcloned into the pET 11a vector and expressed in *Escherichia coli* B834(DE3), a methionine auxotroph (*15*). Expression of the H63M variant was carried out following a procedure similar to that described by Rivera et al. (*16*). In brief, 1.0 L of M9 minimal media supplemented with essential metals (*17*) was inoculated with 5 mL of an *E. coli* B834(DE3) culture grown overnight. When the OD_{600} reached a value of 0.80−1.0, biosynthesis of the polypeptide was induced by adding IPTG (isopropyl-β-thiogalactoside) to a final concentration of 1.0 mM and the culture supplemented with 40 mg of L-methionine per L of fermenting cells. Approximately 10 min after induction of protein synthesis, 17 mg of δ-aminolevulinic acid and 100 mg of $FeSO_4 \cdot 7H_2O$ were added to each liter of cell culture. The cells were harvested by centrifugation 3 h after induction of protein synthesis. Longer incubation times after induction of protein synthesis resulted in the formation of a green color on otherwise reddish cells. The harvested cells were subsequently resuspended and lysed as described previously (*18*). Cell debris was separated by ultracentrifugation, the supernatant made 3 mM in $K_3Fe(CN)_6$, and 1 mM in imidazole, and then dialyzed (Spectrapor; 6−8000 MWCO) at 4.0 °C against ion-exchange buffer (10 mM EDTA, 50 mM Tris, and 1.0 mM imidazole, pH 7.8). The desalted solution was then loaded onto an anion-exchange resin (DE52, Whatman) previously equilibrated with ion-exchange buffer and eluted with a linear salt gradient (0.0 to 0.50 M NaCl) containing 1.0 mM imidazole. Fractions with purity ratio ($A_{280\ nm}/A_{412\ nm}$) < 1.5 were pooled, dialyzed against gel filtration buffer (100 mM NaCl, 20 mM Tris, and 1.0 mM EDTA, pH 7.4), concentrated by ultrafiltration (Y3 Diaflo ultrafiltration membranes, Amicon), and further purified by size-exclusion chromatography (*18*). Fractions with a purity ratio (A_{280}/A_{410}) < 0.5 were pooled, dialyzed exhaustively against 50 mM phosphate buffer, pH 7.0, and concentrated by ultrafiltration to approximately 4−5 mL. Protein concentrations were determined using the molar absorptivity coefficient determined by the pyridine hemochrome method ($\epsilon_{410} = 108\ mM^{-1}\ cm^{-1}$) (*19*).

Electronic Absorption and EPR Spectroscopy. UV−vis spectra of the H63M variant were collected on a Hewlett-Packard 8452A diode array spectrophotometer equipped with a jacketed cuvette holder connected to a thermostated water bath. EPR spectra of samples containing the H63M variant in the presence and in the absence of imidazole (1.0 mM) were acquired using a Bruker EPR spectrometer operating at 9.35 GHz. The samples were analyzed at 4.1 K under the following conditions: receiver gain, 1.0×10^5; microwave power, 0.200 mW; modulation frequency, 100 kHz; modulation amplitude, 5.69 G.

NMR Spectroscopy. Expression and purification of the H63M variant enriched with L-[^{13}C]methyl methionine [$^{13}CH_3SCH_2CH_2CH(NH_2)CO_2H$, Aldrich] was carried out as described above. Proton decoupled ^{13}C-NMR spectra of the H63M variant were obtained at 15 °C with the aid of a *Unity Inova* NMR spectrometer operating at a ^{13}C-spectrometer frequency of 150.57 MHz. The protein solutions (typically 1.5 mM) were exchanged with perdeuterated sodium phosphate buffer ($\mu = 0.10$ M; pH 7.0, not corrected for the isotope effect). In a separate experiment, 1.0 μL of a concentrated imidazole solution was added to the solution containing the variant to achieve a final concentration of 1.0 mM. Typically 3200 scans were collected over a 33 kHz spectral width, with an acquisition time of 0.5 s and a relaxation delay of 1.5 s. The spectra were referenced against an external reference solution consisting of 35% (v/v) of dioxane in D_2O, and processed with a line broadening of 1.5 Hz. The heterocorrelated multiple-quantum coherence (HMQC) (20a) spectrum of the H63M variant in the absence of imidazole was acquired with spectral widths of 18 kHz for ^{1}H and 7 kHz for ^{13}C, a $^1J_{CH}$ set to 140 Hz, water presaturation during the relaxation delay (1.5 s), and WURST decoupling on the ^{13}C channel (20b). The data were collected as an array of 4K × 1K points, which after linear prediction in the t_1 dimension and zero filling in both dimensions produced a 4K × 4K data matrix.

Electrochemistry. Cyclic voltammetry experiments were carried out with a BAS 50W computer-controlled potentiostat. Materials, experimental setup, and methods used in the voltammetric determination of the reduction potentials of the H63M variant were identical to those described by Rivera et al. (21). The voltammetric experiments were typically carried out with solutions consisting of 90 μM protein and 0.20 mM polylysine, in a total volume of 250 μL of MOPS (100 mM, pH 7.0). Transmission mode spectroelectrochemical titrations were carried out in cell bodies constructed of polyacrylate that had an optically transparent gold minigrid (200 wires/in, 70% transmittance, Buckbee Mears Co., St. Paul, MN), quartz windows, a gold minigrid counter electrode, and a compartment for the Ag/AgCl reference electrode. The details of the spectroelectrochemical cell and titrations have been reported elsewhere (*22*). Typical solutions used for these experiments contained 64 μM H63M variant, 50 mM imidazole, and 50 mM phosphate buffer, pH 7.0. Methyl viologen (3.0 mM) and $[Ru(NH_3)_6]Cl_3$ (0.80 mM) were added as mediators. Electronic spectra were taken every 20 mV in the range of −200 to −380 mV vs a Ag/AgCl reference electrode. The spectrum of completely oxidized and completely reduced species were obtained at −100 and −500 mV, respectively.

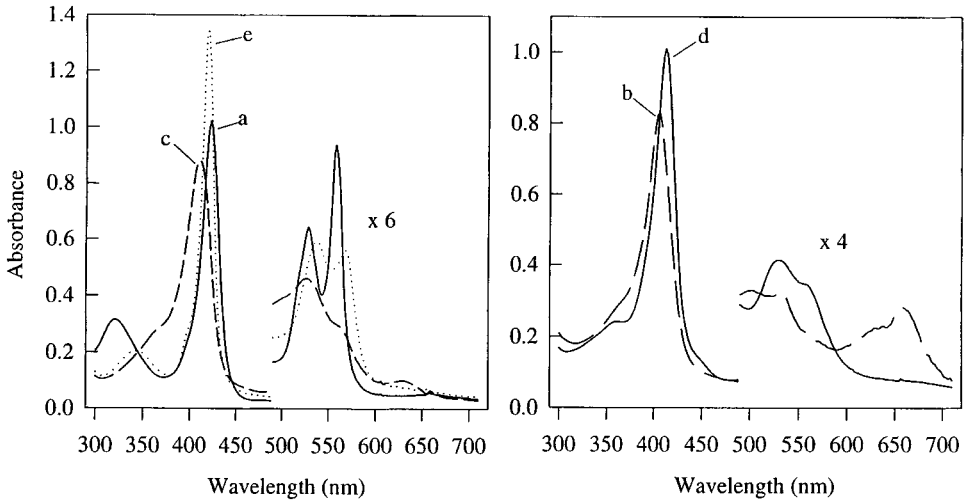

FIGURE 1: Electronic spectra of the H63M variant of OM cyt b_5. (a) Fe(II); (b) Fe(III) species obtained by dialyzing a solution containing the ferrous variant, dithionite (0.10 mM), and dithiothreitol (1.0 mM); (c) Fe(III) species obtained by oxidizing the Fe(II) species with ferricyanide; (d) Fe(III)-imidazole complex. (e) Fe(II)−CO complex.

Coupled Oxidation Assays. Coupled oxidation reactions were carried out at 35 °C with solutions containing 14 μM of the H63M variant in 1.0 mL of 50.0 mM phosphate buffer, pH 7.0. The reaction was initiated by addition of a concentrated solution of sodium ascorbate to achieve a final concentration of 2.0 mM in the reaction mixture, and the reaction was stopped after 7.0 h by cooling to 4.0 °C. An 800 μL aliquot of the resultant solution was extracted with a mixture of pyridine (0.10 mL) and $CHCl_3$ (1.0 mL), and the chloroformic phase was transferred to a test tube, dried over anhydrous Na_2SO_4, concentrated with a gentle stream of nitrogen to approximately 500 μL, and analyzed by UV−vis spectrophotometry.

Mass Spectrometry. The coupled oxidation reaction (10 mL) was performed as described above and stopped after 10 h by cooling to 4 °C. The resultant solution was dialyzed against 40 mM NH_4HCO_3 and subsequently concentrated by ultrafiltration to approximately 600 μL. One hundred microliters of the resultant solution was diluted with 100 μL of 10 mM ammonium acetate and then injected (5 μL/min) into a Sciex API III triple quadrupole mass spectrometer equipped with an atmospheric pressure ion source. Sampling of the positive ions was achieved in the first quadrupole using a voltage difference of 125 V. Increments of 0.1 amu were collected in the range 400−1000 amu.

HPLC Analysis. The regioselectivity of the reaction was assessed by analysis of biliverdin dimethyl ester isomers with the aid of a Beckman System Gold HPLC chromatograph equipped with a diode array UV−vis detector. Samples (dissolved in chloroform) were prepared as follows. A solution containing the reaction product (10 mL) was extracted with a mixture of 2-picoline (2.0 mL) and $CHCl_3$ (5.0 mL). The conversion of verdoheme to biliverdin was accomplished by addition of KOH followed by the addition of HCl to the chloroformic phase, as described by Saito and Itano (*23*). Synthesis of the dimethyl esters was carried out as described by O'Carra and Colleran (*24*). Coupled oxidation of the pyridine hemochrome was carried out as described by Torpey and Ortiz de Montellano (*25*). Samples were injected into a Beckman Ultrasphere ODS C18 column (4.6 mm × 25 cm) and separated by isocratic elution with a mixture 20:80 consisting of methanol:methanol/water (75/25). The retention time of the product generated from the coupled oxidation of the heme in the H63M variant was compared to those obtained from samples of authentic α-biliverdin (Sigma), and from samples obtained by coupled oxidation of iron protoporphyrin IX in the presence of pyridine.

RESULTS

Protein Purification and Electronic Spectra. Centrifugation of the B834(DE3) cells 3 h after induction of protein synthesis produces a red pellet due to the overexpression of the OM cyt b_5 variant. After lysis and ultracentrifugation, the mutant is in the reduced state, as indicated by its visible spectrum (Figure 1a), and it oxidizes upon dialysis. When the H63M variant is oxidized during the dialysis process, its electronic spectrum (Figure 1b) displays a band at 660 nm. On the other hand, when the protein is oxidized with an excess of potassium ferricyanide in the presence of imidazole, immediately after ultracentrifugation, the spectrum of the resultant ferric protein is devoid of the band at 660 nm (Figure 1c). These results provided the first indication that the ferrous H63M variant reacts with oxygen to produce a derivative whose electronic spectrum displays a peak at 660 nm. The electronic spectrum of the ferric variant displays a charge-transfer transition at 630 nm (Figure 1c) indicative of a high-spin state. The spin state of the ferric variant was corroborated by its EPR spectrum which displays signals with g values at 6.45 and 2.16 (*26*), typical of high-spin ferric hemes with histidine as the proximal ligand. On the other hand, the ferrous protein appears to be in the low-spin state, as indicated by the resolved α- and β-bands (558 and 528 nm, respectively) observed in its electronic spectrum (Figure 1a). Furthermore, when CO is bubbled through a solution of the ferrous variant, a stable Fe^{2+}−CO species is formed, as indicated by its electronic spectrum (Figure 1e).

When a solution containing the ferric protein was loaded onto an ion-exchange column, a red band was formed at the top of the column, as expected. However, when the salt gradient was started, the characteristic red color of the holoprotein disappeared gradually, leaving behind a green color characteristic of heme devoid of axial ligands. This

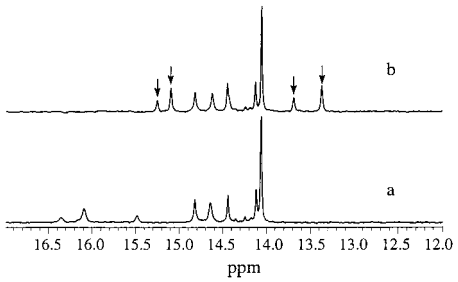

FIGURE 2: ^{13}C-NMR spectrum of the H63M variant labeled with L-^{13}C-methyl methionine. (a) Fe(III); (b) Fe(III)−imidazole complex. Resonances not arising from Met 63 in spectrum (a), i.e., those observed in the range between 14.00 and 14.90 ppm, do not shift upon formation of the Fe(III)−imidazole complex. Resonances highlighted with arrows arise from Met-63 upon formation of the Fe(III)−imidazole complex.

indicated that the ferric variant loses its heme during the elution process, presumably due to electrostatic interactions between the heme propionates and the anion-exchange resin. This suggests that the heme−H63M complex is significantly weaker than the heme-wild-type cyt b_5 complex. To purify the holoprotein by ion-exchange chromatography, the solution containing the ferric H63M variant was made 1.0 mM in imidazole and then loaded onto an ion-exchange column, previously equilibrated with ion-exchange buffer containing 1 mM imidazole. The holoprotein was eluted, subsequently dialyzed in order to remove the imidazole, and then purified by size-exclusion chromatography. The electronic spectrum of the ferric H63M−imidazole complex (Soret band at 412 nm and a visible peak at 530 nm) (Figure 1d) is similar to that obtained from wild-type OM cyt b_5, hence suggesting that the heme becomes hexacoordinated in the presence of imidazole. The incorporation of imidazole as the sixth ligand was corroborated from the EPR spectrum of the H63M−imidazole complex, which displays signals with g values characteristic of low-spin ferric hemoproteins, $g = 3.04$, 2.22, and 1.45.

NMR Spectroscopy. To determine whether Met-63 binds to the ferric heme, the H63M variant was expressed in *E. coli* B834(DE3), a methionine auxotroph. This strategy permitted the labeling of the variant with ^{13}C-methyl methionine. The ^{13}C-NMR spectrum of the labeled variant (Figure 2a) displays eight resonances between 13.90 and 16.50 ppm. These resonances arise from Met-1, Met-23, Met-63, and Met-70. On the basis of ^{1}H-NMR spectroscopic studies, it has been previously demonstrated that cyt b_5 is a mixture of two interconvertible isomers that differ by a 180° rotation about the $\alpha-\gamma$-meso axis of the heme (*27*). The ratio of isomeric populations A:B in the case of OM cytochrome b_5 is 1:1 (*28*). It is also known from the crystal structure of OM cyt b_5 (*16*) that the side chain of Met-23 is in van der Waals contact with the heme substituents on pyrrole I, and that Met-80 is in van der Waals contact with the heme substituents on pyrrole III. On this basis, it is possible to propose that the intense signal at 14.06 ppm (Figure 2a) arises from Met-1, while the two sets of resonances at 14.11, 14.45 and 14.64, 14.82 ppm originate from Met-23 and -70. Each set consists of two resonances of almost equal intensity due to the heme isomeric mixture A:B = 1:1. The three resonances between 15.40 and 16.50 ppm appear to arise from Met-63. The relatively larger width of these resonances seems to indicate that their corresponding

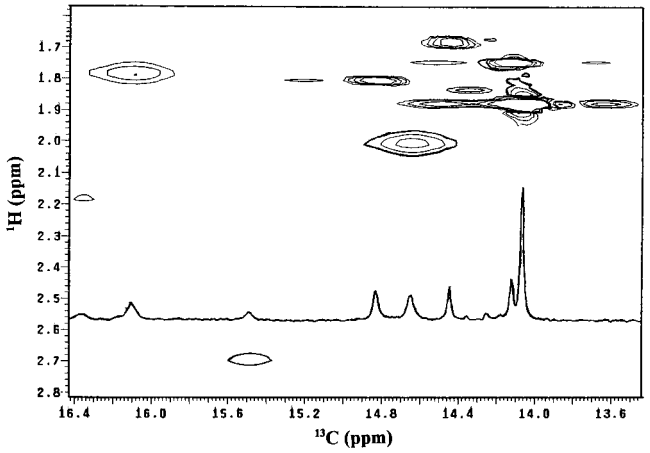

FIGURE 3: HMQC spectrum of the H63M variant labeled with L-[^{13}C]methyl methionine.

methyl groups are in relative close proximity to the ferric ion, hence favoring dipolar interactions with the unpaired electron on the ferric heme. It is noteworthy, however, that the chemical shift range observed for the methyl carbons in all methionine residues is typical of methyl carbons in diamagnetic molecules. This implies that the sulfur atom in Met-63 is not coordinated to the ferric heme iron.

Addition of imidazole to a solution of the variant results in large shifts for the resonances arising from Met-63. The position of the resonances arising from Met-63 in the H63M−imidazole complex is highlighted by arrows in Figure 2b. There are four resonances arising from Met-63 because there are two orientations of the methionine and two orientations of the heme in the active site. Furthermore, these resonances become narrower upon binding of exogenous imidazole, hence suggesting a weaker dipolar interaction between the methyl carbons and the unpaired electron on the heme iron. This indicates that the methyl group in Met-63 is displaced further away from the heme iron upon binding of imidazole. In contrast, the resonances between 13.90 and 14.80, which are thought to arise from Met-1, Met-23, and Met-70, are not affected (Figure 2b). Additional evidence that Met-63 is not bound to the ferric heme was obtained from the ^{1}H chemical shifts arising from the methyl groups in the H63M variant. These ^{1}H chemical shifts, which were obtained with the aid of an HMQC experiment (Figure 3), are characteristic of methyl groups in diamagnetic environments, thus clearly indicating that Met 63 is not bound to the ferric heme.

Electrochemistry. The reduction potential of the H63M variant was measured by spectroelectrochemistry and by cyclic voltammetry in the presence and in the absence of imidazole. A family of spectra obtained during the spectroelectrochemical titration of the variant in the presence of imidazole is shown in Figure 4, along with the Nernst plot (inset). The reduction potential of the imidazole−H63M complex, which was shown to exist as a low-spin Fe(III) species, was found to be −92 mV vs NHE. The reduction potential of this species measured by cyclic voltammetry was found to be −80 mV vs NHE (Figure 5a). By comparison, the reduction potential of OM cyt b_5 (a bis-histidine coordinated species) measured potentiometrically under similar conditions is −102 mV vs NHE (*29*). The spectroelectrochemical measurement of the reduction potential

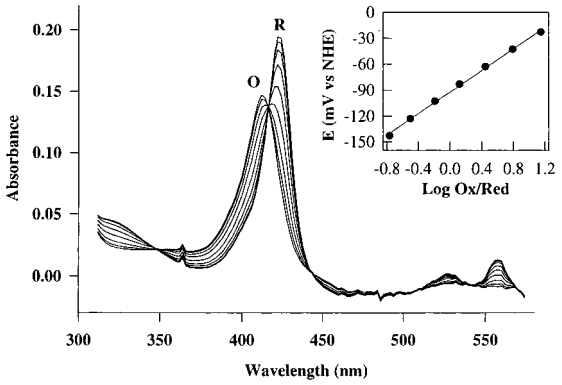

FIGURE 4: Spectroelectrochemical titration of solutions containing the H63M variant (64 μM) in the presence of imidazole (50 mM). (Inset) Nernst plot constructed from the dependence of the absorbance at 424 nm on the applied potential. The Nernst slope is 62 mV.

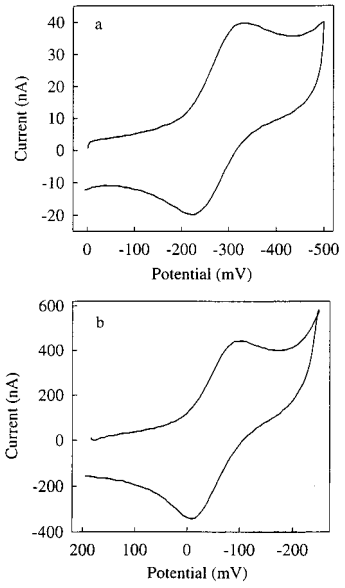

FIGURE 5: Cyclic voltammograms obtained from solutions containing the H63M variant of OM cyt b_5 (90 μM), in the presence (a) and in the absence (b) of imidazole (50 mM). A gold disk electrode was modified with β-mercaptopropionate and the voltammogram was obtained in the presence of 0.20 mM polylysine (MW = 3970), with a scan rate of 20 mV/s. The potential axis shown is with respect to the Ag/AgCl reference electrode but the reduction potentials in the text are given with respect to the NHE.

exhibited by the H63M variant in the absence of imidazole was more difficult to obtain due to the gradual decomposition of the protein during the course of the potentiometric titration. The reduction potential obtained for the variant from several potentiometric measurements is 110 mV vs NHE. To substantiate this value, its reduction potential was measured by cyclic voltammetry (Figure 5b) and found to be +130 mV vs NHE. It has been previously reported that when electrodes modified with polyelectrolytes are utilized for voltammetric measurements of the reduction potential of cytochrome b_5, the observed values are consistently more positive than those measured potentiometrically (*21*, *29*). An explanation for the observed anodic shifts has been proposed recently (*21*). Consequently, the value of the reduction potential measured potentiometrically for the H63M variant (110 mV), appears to be reasonably close to the true value. It is also noteworthy that this value compares well with the reduction potential displayed by horse heart myoglobin, 45 mV (*30*), sperm whale myoglobin, 55 mV (*31*), and human myoglobin, 50 mV (*31*), consistent with a species in which heme is axially ligated by a proximal histidine.

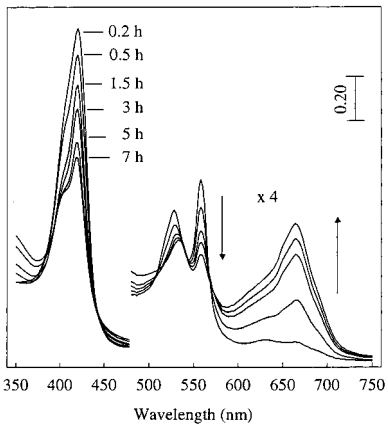

FIGURE 6: Changes in the electronic spectrum of the H63M variant of OM cyt b_5 during the coupled oxidation of heme in the presence of ascorbate.

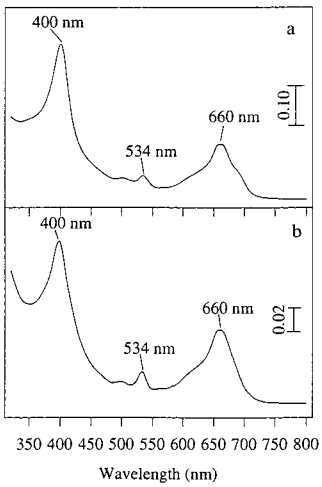

FIGURE 7: (a) Electronic spectrum of a solution containing the H63M-verdoheme complex obtained after 7 h of reaction with ascorbate. (b) Electronic spectrum of the verdohemochrome obtained by extracting the verdoheme in solution (a) with 10% pyridine in chloroform.

Coupled Oxidation of Heme. The addition of excess ascorbate to a solution of the H63M variant previously equilibrated with air was monitored spectrophotometrically (Figure 6). The electronic spectrum of the ferric H63M variant before addition of ascorbate was identical to that shown in Figure 1c. Addition of ascorbate results in reduction of the variant, as demonstrated by the Soret band (420 nm) and visible peaks at 558 and 528 nm that are characteristic of a hexacoordinated low-spin ferrous heme. As the coupled oxidation reaction proceeds, the intensity of the Soret band at 420 nm decreases with the concomitant increase of a peak at 402 nm. The peaks at 528 and 558 nm also disappear, giving rise to a peak with absorption maxima at 534 nm. It is also evident from Figure 6 that as the reaction progresses, a peak with absorption maxima at 660 nm is formed, whose intensity increases as the reaction proceeds. The electronic spectrum obtained after 7.0 h of reaction (Figure 7a) is very similar to the spectrum reported for the pyridine hemochrome of verdoheme (*32*), therefore implying that verdoheme is the product of the coupled

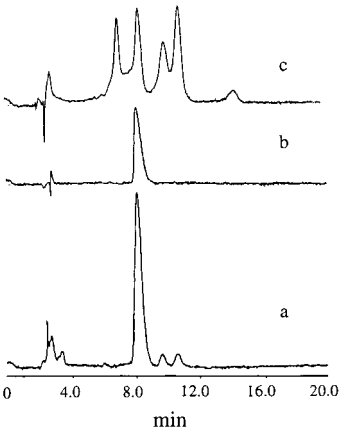

FIGURE 8: Chromatograms obtained from solutions containing the dimethyl ester derivatives of (a) biliverdin obtained from the verdoheme that is formed upon coupled oxidation of the heme in the H63M variant, (b) standard biliverdin, and (c) biliverdin obtained from a coupled oxidation reaction of iron protoporphyrin IX in aqueous pyridine.

oxidation reaction performed by the H63M variant of OM cytochrome b_5.

Additional evidence corroborating that verdoheme is the product of the coupled oxidation of the heme in the H63M variant of OM cyt b_5 was obtained by incubating a more concentrated solution of the variant with ascorbate. The reaction was stopped after approximately 10 h and the reaction product extracted as the pyridine hemochrome into chloroform. The electronic spectrum obtained from the resultant chloroform solution (Figure 7b) is identical to the spectrum reported by Lagarias (*32*) for the pyridine hemochrome of verdoheme. Moreover, in a separate experiment, the coupled oxidation reaction was quenched by cooling the reaction mixture to 4.0 °C. The ascorbate-containing solution of the variant was subsequently dialyzed vs a 40 mM solution of ammonium bicarbonate at 4.0 °C. The resultant solution was concentrated by ultrafiltration, diluted with ammonium acetate and analyzed by electrospray mass spectrometry. The resultant mass spectrum displays a small peak corresponding to unmodified heme ($m/z = 616$), and a large peak corresponding to verdoheme ($m/z = 619$), thus conclusively demonstrating that the product of the coupled oxidation performed by the H63M variant is verdoheme.

Regioselectivity of the Coupled Oxidation Reaction. The regiospecificity of the reaction performed by the H63M variant was assessed by extracting the verdoheme produced upon coupled oxidation into 2-picoline, hydrolyzing it to iron-biliverdin in basic picoline, followed by acidification of the picoline solution in order to produce biliverdin (*23*). The biliverdin was then esterified with methanol and the resultant dimethyl ester derivative analyzed by HPLC. The chromatogram obtained for the sample derived from the coupled oxidation performed by the H63M variant (Figure 8a) shows a peak with retention time of approximately 8.0 min. A sample of biliverdin dimethyl ester (Figure 8b), which was derived from α-biliverdin, displays a peak with retention time identical to that observed for the product of the coupled oxidation performed by the variant. This is strong evidence suggesting that the coupled oxidation performed by the variant is regioselective, with oxygen attacking the α-meso position, as is observed in the case of myoglobin and heme oxygenase. In a separate experiment, the pyridine hemochrome was incubated with ascorbate. It is known that during the coupled oxidation of the pyridine hemochrome, all four meso positions are attacked by oxygen to produce a random mixture of isomeric biliverdins (*33*, *34*). The chromatogram obtained from a sample derived from the coupled oxidation of the pyridine hemochrome displays four peaks with retention times ranging 6.0−12.0 min (Figure 8c). This experiment demonstrates that the four isomeric biliverdins can be separated with the conditions utilized in the analysis of the reaction products by HPLC. Consequently, it can be concluded that the coupled oxidation of heme performed by the H63M variant occurs with >90% regioselectivity for the α-meso position.

DISCUSSION

Sligar and Egeberg (*35*) replaced histidine-39, a heme axial ligand in rat microsomal cyt b_5 for a methionine. On the basis of EPR and resonance Raman spectroscopic studies, these authors reported that the ferric form is a six-coordinated high-spin species. These authors also reported that it was not possible to conclude whether Met-39 or a water molecule act as the sixth axial ligand in the ferric H39M variant of microsomal cyt b_5. The reduction potential of this protein was found to be −240 mV vs NHE (*35*), as compared with 6 mV for the wild-type protein (*36*). Furthermore, the H39M variant of rat microsomal cyt b_5 was found to catalyze intermolecular oxidative reactions, demonstrated with the hydrogen peroxide-dependent oxidative demethylation of *N*,*N*-dimethylaniline (*35*). On the other hand, when His-63, the other axial ligand in microsomal cytochrome b_5 was mutated to a methionine, the apoprotein failed to incorporate heme during cell fermentation (*37*).

By comparison, the evidence presented in this report demonstrates that the H63M variant of outer mitochondrial membrane (OM) cyt b_5 exists as a high-spin ferric species coordinated by a proximal histidine residue (His-39), and likely, by a distal water (discussed below). NMR spectroscopic studies provided strong evidence indicating that Met-63 is not coordinated to the ferric heme iron. The reduction potential of the H63M variant of OM cyt b_5 was found to be +110 mV vs NHE, a value in close agreement to that displayed by myoglobin. It is also noteworthy that the mitochondrial H63M variant performs an efficient intramolecular oxidative reaction, the coupled oxidation of heme. On the other hand, the H39M variant of OM cyt b_5 does not incorporate heme during cell fermentation.

Heme Axial Ligation. The EPR and electronic spectra of the ferric H63M variant of OM cyt b_5 are similar to those displayed by met-aquomyoglobin (*38*), indicating that the heme in the ferric variant may be coordinated by His-63 in the proximal side and by water in the distal pocket. Coordination of water in the distal pocket of the ferric variant can be inferred from the band at 630 nm that is observed in its electronic spectrum. In myoglobin, this band has been assigned to an Fe−O charge-transfer transition (*38*). When imidazole is added to a solution of the ferric H63M variant, the resultant electronic spectrum (Figure 1d) is very similar to that displayed by ferric OM cyt b_5 (*28*), with Soret band at 412 nm and visible peaks at 530 and 556 nm. It is therefore possible to suggest that the exogenous imidazole coordinates the heme iron in the distal site, producing a ferric

low-spin species, as manifested by the disappearance of the band at 630 nm (Figure 1d). Consistent with coordination of the heme by a proximal histidine, the reduction potential of the H63M variant in the absence of imidazole was found to be 110 mV vs NHE, a value that is in good agreement with the reduction potentials observed for myoglobin. Also consistent with the proposed heme axial ligation, the reduction potential of the variant measured in the presence of imidazole is −90 mV vs NHE. This value is in good agreement with the $E°$ measured for the bis-histidine coordinated OM cyt b_5, −102 mV (*29*), implying that His-39 coordinates in the proximal site and exogenous imidazole coordinates in the distal pocket. It is important to note, however, that the electronic spectrum of the reduced species (Figure 1a) shows well-resolved α- and β-bands at 558 and 528 nm, respectively, and a Soret band at 424 nm. This spectrum is indicative of a low-spin Fe^{2+} species, hence indicating that, upon reduction, the heme is coordinated by His-39 and by Met-63.

Conclusive evidence indicating that Met-63 does not coordinate the heme in the ferric variant was obtained from NMR spectroscopic studies performed with ^{13}C-methyl methionine- labeled protein. The ^{1}H and ^{13}C chemical shifts arising from the methyl groups in all four Met residues of the ferric H63M variant resonate in their expected diamagnetic region, 13.0−17.0 ppm for ^{13}C and 1.80−2.90 ppm for ^{1}H (Figures 2 and 3). Coordination of Met-63 to the ferric ion of the heme should result in the observation of contact shifts for the ^{1}H and ^{13}C nuclei in the methyl group of Met-63. These contact shifts are a consequence of unpaired electron density originating from the ferric ion which is delocalized into the methionine side chain via the S−Fe coordinative bond. In fact, this is observed in the case of cytochrome *c*, where the Met-80 methyl protons resonate at −21 ppm (*39*). In summary, the evidence discussed above indicates that the ferric variant is coordinated by His-39 in the proximal side and by water in the distal side, whereas the corresponding ferrous species appears to be coordinated by His-39 and Met-63.

Coupled Oxidation of Heme. Heme catabolism is carried out by the enzyme heme oxygenase (HO) via the NADPH-dependent cleavage of heme to biliverdin and carbon monoxide (*40*). The heme oxygenase reaction proceeds via a sequential mechanism in which catalytic turnover of HO requires NADPH-cytochrome P450 reductase as a source of reducing equivalents and molecular oxygen (*40*−*43*). The catalytic cycle of heme oxygenase (Figure 9) parallels that of cytochrome P450 in that an oxyferrous complex is formed which accepts a second electron from cytochrome P450 reductase in order to form an activated oxidizing species (*44*). The activated oxidizing species in HO adds a hydroxyl to the heme α-meso position, thus producing α-hydroxyheme (*45*), which undergoes a subsequent O_2-dependent elimination of the hydroxylated α-meso carbon as CO, with the concomitant formation of α-verdoheme (Figure 9). Finally, α-verdoheme is cleaved in an NADPH- and O_2-dependent manner to produce α-biliverdin (*23*, *46*). A related reaction is that of coupled oxidation, in which heme is reacted with a reducing agent, usually ascorbate or hydrazine, and molecular oxygen (*47*). The coupled oxidation of heme produces biliverdin via the formation of intermediate species such as hydroxyheme and verdoheme, as shown in Figure 9

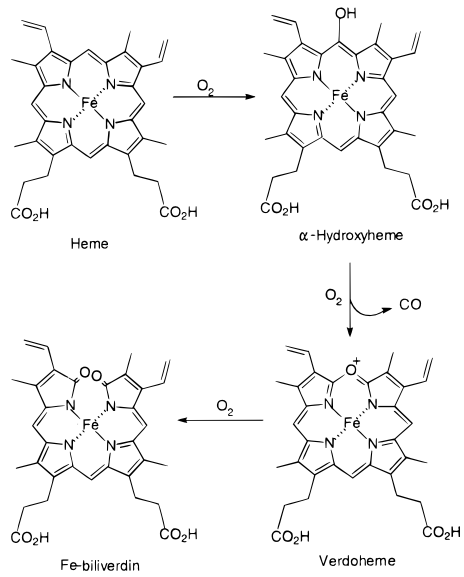

FIGURE 9: Schematic representation of the reaction pathway for the conversion of protoporphyrin IX into Fe-α-biliverdin by heme oxygenase.

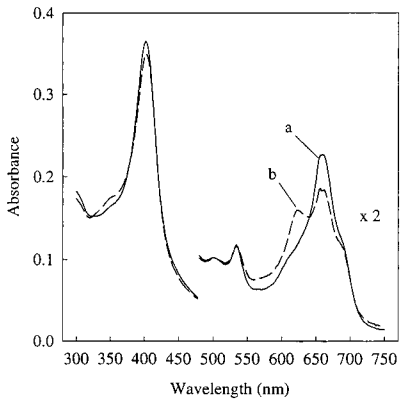

FIGURE 10: Electronic spectra obtained from the product of the coupled oxidation reaction of the heme in the H63M variant (a) before, and (b) after saturating the solution with carbon monoxide.

for the reaction catalyzed by HO. Whereas the coupled oxidation of free heme in aqueous pyridine produces a random mixture of four biliverdin isomers, the coupled oxidation of heme in heme proteins is regioselective. For example, coupled oxidation of heme in myoglobin yields almost exclusively α-biliverdin, whereas human hemoglobin yields 60% α-biliverdin, and 40% β-isomer (*14*, *34*, *48*). Incubation of the H63M variant of OM cytochrome b_5 with ascorbate results in the formation of >90% α-verdoheme, as demonstrated by its electronic spectrum (Figure 7), by electrospray mass spectrometry, and by HPLC analysis (Figure 8).

The formation of verdoheme and not iron-biliverdin upon coupled oxidation of the heme in the H63M variant may arise from the formation of a hexacoordinated (His−Met) ferrous−verdoheme−protein complex. The formation of a hexacoordinated species can be inferred from the electronic spectrum arising from the product obtained by incubating the H63M variant with a 100-fold excess of ascorbate (Figure 10a). This spectrum displays a band at 660 nm which is almost identical to the one observed in the electronic spectrum of the ferrous pyridine hemochrome of verdoheme (*32*). By comparison, the electronic spectrum of the ferrous

pentacoordinated verdoheme in heme oxygenase displays a band at 690 nm (*45*). These observations suggest that molecular oxygen cannot readily displace Met-63 from its coordination site on verdoheme, hence arresting the coupled oxidation reaction at the verdoheme stage. Consequently, the mechanism of inhibition for the oxidation of verdoheme to iron-biliverdin in the H63M variant is similar to that observed for turnover of the heme−heme oxygenase complex in the presence of carbon monoxide (*49*, *50*), and is consistent with the proposal that further oxygenation of verdohemochrome to iron-biliverdin occurs only with pentacoordinated verdoheme complexes (*51*). In a similar fashion, ligands that bind both the fifth- and sixth-coordination sites of verdoheme with relatively high affinity inhibit the formation of biliverdin from verdoheme (*23*).

Additional evidence for the relatively strong coordination bond formed between Met-63 and the verdoheme iron was obtained from a solution containing the product formed upon incubating the H63M variant with ascorbate. The electronic spectrum of the reaction product, H63M−verdoheme complex, is shown in Figure 10a. When this solution was saturated with CO, the band at 660 nm decreased in intensity, with a concomitant increase in the intensity of a new band at 635 nm (Figure 10b). The latter arises from verdoheme coordinated by His-39 and CO (*46*, *49*, *50*). It is noteworthy that the band at 660 does not disappear completely upon saturating the solution with CO for 20 min. However, when air is bubbled to displace the carbon monoxide, the band at 635 disappears and the intensity of the band at 660 nm increases to yield the original spectrum (Figure 10a). By comparison, when a solution of the ferrous H63M variant (Figure 1a) was bubbled with CO, the carbomonoxy complex (Figure 1b) is formed immediately. These observations taken together imply that the H63M complex is capable of activating oxygen in order to perform the oxygenation of heme. On the other hand, Met-63 coordinated to the verdoheme iron in the H63M variant is not readily displaced by CO. Consequently, it is likely that Met-63 cannot be displaced by O_2 from its coordination site on verdoheme, which is consistent with the fact that the coupled oxidation of heme in the H63M variant is arrested at the verdoheme stage.

Concluding Remarks. Heme oxygenase catalyzes the NADPH- and cytochrome-P450-reductase-dependent oxidation of heme to biliverdin and carbon monoxide (*40*). It has been proposed that carbon monoxide generated by the heme oxygenase system functions as an important second-messenger molecule (*52*, *53*). Therefore, the detailed understanding of the mechanism by which heme oxygenase converts heme to biliverdin is of important physiological relevance. Although several important advances have been made toward the understanding of the mechanism by which heme oxygenase activates heme, important issues such as the details of oxygen activation are not fully resolved yet. Furthermore, it has been suggested that the mechanism of oxygen activation displayed by heme oxygenase appears to be different from the mechanism displayed by cytochromes P450 and peroxidases (*50*, *54*, *55*). Additional progress in this area has been difficult due to the lack of a three-dimensional structure for heme oxygenase. It has also been proposed that understanding the detailed mechanistic aspects of the coupled oxidation reaction performed by myoglobin and other heme-containing proteins is likely to shed light into the details of oxygen activation performed by heme oxygenase (*14*). The evidence presented in this report indicates that further research with the H63M and related variants of OM cyt b_5 may provide important insights related to the mechanistic aspects of heme oxygenation performed by heme oxygenase. In comparison to other heme-containing proteins known to undergo coupled oxidation, the heme in cyt b_5 is largely exposed to the aqueous environment. In addition, the heme-binding affinity exhibited by the H63M variant appears to be lower than that exhibited by the wild-type protein. These structural properties compare well with those postulated for the active site in heme oxygenase, which is thought to bind heme with lower affinity and with larger exposure to the aqueous environment than observed for most heme-containing proteins.

ACKNOWLEDGMENT

We wish to express our gratitude to Professor F. Ann Walker for her assistance with the EPR spectra. The electrospray-mass spectrometric experiments were performed at the Molecular Biology Resource Facility at the William K. Warren Medical Research Institute, Oklahoma City, OK.

REFERENCES

1. Ortiz de Montellano, P. R. (1987) *Acc. Chem. Res. 20*, 289−294.
2. Raphael, A. L., and Gray, H. B. (1989) *Proteins: Struct., Funct., Genet. 6*, 338−340.
3. Raphael, A. L., and Gray, H. B. (1991) *J. Am. Chem. Soc. 113*, 1038−1040.
4. Lloyd, E., Hildebrand, D. P., Tu, K. M., and Mauk, A. G. (1995) *J. Am. Chem. Soc. 117*, 6434−6438.
5. Barker, P. D., Nerou, E. P., Cheesman, M. R., Thomson, A. J., Oliveira, P., and Hill, H. A. O. (1996) *Biochemistry 35*, 13618−13626.
6. Barrick, D. (1994) *Biochemistry 33*, 6546−6554.
7. Adachi, S., Nagano, S., Watanabe, Y., Ishimori, K., and Morishima, I. (1991) *Biochem. Biophys. Res. Commun. 180*, 138−144.
8. Adachi, S., Nagano, S., Ishimori, K., Watanabe, Y., Morishima, I., Egawa, T., Kitagawa, T., and Makino, R. (1993) *Biochemistry 32*, 241−252.
9. Mus, I., Dolla, A., Guerlesquin, F., Payan, F., Czjek, M., Haser, R., Bianco, P., Haladjian, J., Rapp, B. J., Wall, J. D., Voordouw, G., and Bruschi, M. (1992) *J. Biol. Chem. 267*, 16851−16858.
10. Ferrer, J. C., Guillemette, J. G., Bogumil, R., Inglis, S. C., Smith, M., and Mauk, A. G. (1993) *J. Am. Chem. Soc. 115*, 7507−7508.
11. Dolla, A., Florens, L., Bianco, P., Haladjian, J., Voordouw, G., Forest, E., Wall, J., Guerlesquin, F., and Bruschi, M. (1994) *J. Biol. Chem. 269*, 6340−6346.
12. Thodorakis, J. L., Barber, E. A. E., McCracken, J., Peisach, J., Schejter, A., and Margoliash, E. (1995) *Biochim. Biophys. Acta 1252*, 103−113.
13. Schejter, A., Galia, T., Navon, G., Liu, X. J., and Margoliash, E. (1996) *J. Am. Chem. Soc. 118*, 477−478.
14. Hildebrand, D. P., Tang, H., Luo, Y., Hunter, C. L., Smith, M., Brayer, G. D., and Mauk, A. G. (1996) *J. Am. Chem. Soc. 118*, 12909−12915.
15. Doherty, A. J., Ashford, S. R., Brannigan, J. A., and Wigley, D. B. (1995) *Nucleic Acids Res. 23*, 2074−2075.
16. Rodríguez-Marañón, M. J., Qiu, F., Stark, R. E., White, S. P., Zhang, X., Foundling, S. I., Rodríguez, V., Schilling, C. L., III, Bunce, R. A., and Rivera, M. (1996) *Biochemistry 35*, 16378−16390.

17. One liter of minimal media consisted of the following: $Na_2HPO_4 \cdot 7H_2O$ (47.7 mM), KH_2PO_4 (22.0 mM), NaCl (8.55 mM), NH_4Cl (18.7 mM), nitrilotriacetic acid (1.00 mM), $MgSO_4$ (2.00 mM), $CaCl_2$ (0.100 mM), $(NH_4)_6Mo_7O_{24} \cdot 4H_2O$ (0.150 μM), $FeSO_4 \cdot 7H_2O$ (40.0 μM), EDTA (17.0 μM), $CuSO_4 \cdot 5H_2O$ (3.00 μM), $Co(NO_3) \cdot 6H_2O$ (2.00 μM), $Zn(SO_4) \cdot 7H_2O$ (7.60 μM), $Na_2B_4O_7 \cdot 10H_2O$ (9.40 μM), ampicillin (0.270 mM), D-(+)-glucose (27.7 mM), and L-methionine (0.268 mM).
18. Rivera, M., and Walker, F. A. (1995) *Anal. Biochem. 230*, 295−302.
19. de Duve, C. (1948) *Acta Chem. Scand. 2*, 264−269.
20. (a)Summers, M. F., Marzilli, L. G., and Bax, A. (1986) *J. Am. Chem. Soc.* 108, 4285−4294; (b) Kupće, E., and Freeman, R. (1995) *J. Magn. Reson*. *115*A, 273−276.
21. Rivera M., Seetharaman, R., Girdhar, D., Wirtz, M., Zhang, X., Wang, X., and White, S. (1998) *Biochemistry 37*, 1485−1494.
22. Walker, F. A., Emrick, D., Rivera, J. E., Hanquet, B. J., and Buttlaire, D. H. (1988) *J. Am. Chem. Soc. 110*, 6234−6240.
23. Saito, S., and Itano, H. A. (1982) *Proc. Natl. Acad. Sci. U.S.A. 79*, 1393−1397.
24. O'Carra, P., and Colleran, E. (1970) *J. Chromatogr. 50*, 458−468.
25. Torpey, J., and Ortiz de Montellano, P. R. (1996) *J. Biol. Chem. 271*, 26067−26073.
26. Rodríguez, J. C., Desilva, T., and Rivera, M. (1998) *Chem. Lett.* 353−354.
27. (a) Keller, R. M., & Wütrhrich, K. (1980) *Biochim. Biophys. Acta 621*, 204−217; (b) La Mar, G. N., Burns, P. D., Jackson, J. T., Smith, K. M., Langry, K. C. and Strittmatter, P. (1981) *J. Biol. Chem. 256*, 6075−6079.
28. Rivera, M., Barillas-Mury, C., Christensen, K. A., Little, J. W., Wells, M. A., and Walker, F. A. (1992) *Biochemistry 31*, 12233−12240.
29. Rivera, M., Wells, M. A., and Walker, F. A. (1994) *Biochemistry 33*, 2161−2170.
30. Hildebrand, D. P., Burk, D. L., Maurus, R., Ferrer, J. C., Brayer, G. D., and Mauk, A. G. (1995) *Biochemistry 34*, 1997−2005.
31. Varadarajan, R., Zewert, T. E., Gray, H. B., Boxer, S. G. (1989) *Science 243*, 69−72.
32. Lagarias, J. C. (1982) *Biochim. Biophys. Acta 717*, 12−19.
33. Petryka, Z., Nicholson, D. C., and Gray, C. H. (1962) *Nature 194*, 104.
34. O'Carra, P., and Colleran, E. (1969) *FEBS Lett. 5*, 295−298.
35. Sligar, S. G., and Egeberg, K. (1987) *J. Am. Chem. Soc. 109*, 7896−7897.
36. Rodgers, K. K., and Sligar, S. G. (1991) *J. Am. Chem. Soc. 113*, 9419−9421.
37. Beck von Bodman, S., Schuler, M. A., Jollie, D. R., and Sligar, S. G. (1986) *Proc. Natl. Acad. Sci. U.S.A. 83*, 9443−9447.
38. Antonini, E., and Brunori, M. (1971) in *Hemoglobin and Myoglobin in their Reactions with Ligands* (Neuberger, A., and Tatum, E. L., Eds.) pp 13−39, North-Holland Publishing Co., Amsterdam.
39. Feng, Y., Roder, H., and Englander, S. W. (1990) *Biophys. J. 57*, 15−22.
40. Tenhunen, R., Marver, H. S., and Schmid, R. (1969) *J. Biol. Chem. 244*, 6388−6394.
41. Brown, S. B., and King, R. F. G. (1976) *Biochem. Soc. Trans. 4*, 197−201.
42. Yoshida, T. and Kikuchi, G. (1978) *J. Biol. Chem. 253*, 4224−4229.
43. Yoshida, T. and Kikuchi, G. (1978) *J. Biol. Chem. 253*, 4230−4236.
44. Yoshida, T. Noguchi, M., and Kikuchi, G. (1980) *J. Biol. Chem. 255*, 4418−4420.
45. Liu, Y., Moënne-Loccoz, P., Loehr, T. M., and Ortiz de Montellano, P. R. (1997) *J. Biol. Chem. 272*, 6909−6917.
46. Yoshida, T., and Noguchi, M. (1984) *J. Biochem. 96*, 563−570.
47. Brown, S. B., Chabot, A. A., Enderby, E. A., and North, A. C. T. (1981) *Nature 289*, 93−95.
48. Brown, S. B. (1976) *Nature 159*, 23−27.
49. Yoshida, T., Noguchi, M., and Kikuchi, G. (1980) *J. Biochem. 88*, 557−563.
50. Wilks, A., and Ortiz de Montellano, P. R. (1993) *J. Biol. Chem. 268*, 22357−22362.
51. Sano, S., Sano, T. Morishima, I., Shiro, Y., and Maeda, Y. (1986) *Proc. Natl. Acad. Sci. U.S.A. 83*, 531−535.
52. Verma, A., Hirsch, D. J., Glatt, C. E., Ronnett, G. V., and Snyder, S. H. (1993) *Science 259*, 381−384.
53. (a) Maines, M. D. (1997) *Annu. Rev. Pharmacol. Toxicol.* 37, 517−554; (b) Maines, M. D. (1993) *Mol. Cell. Neurosci. 4*, 389−397.
54. Takahasi, S., Ishikawa, K., Takeuchi, N., Ikeda-Saito, M., Yoshida, T., and Rousseau, D. (1995) *J. Am. Chem. Soc. 117*, 6002−6006.
55. Hernández, G., Wilks, A., Paolesse, R., Smith, K. M., Ortiz de Montellano, P. R., and La Mar, G. (1994) *Biochemistry 33*, 6631−6641.

BI9809324